Soft x-ray free-electron laser induced damage to inorganic scintillators

Tomáš Burian,[1,2*] Věra Hájková,[1] Jaromír Chalupský,[1] Luděk Vyšín,[1] Pavel Boháček,[1] Martin Přeček,[1] Jan Wild,[2] Cigdem Özkan,[3,4] Nicola Coppola,[4] Shafagh Dastjani Farahani,[4] Joachim Schulz,[4,7] Harald Sinn,[4] Thomas Tschentscher,[4] Jérôme Gaudin,[5] Saša Bajt,[6] Kai Tiedtke,[6] Sven Toleikis,[6] Henry N. Chapman,[7,8] Rolf A. Loch,[7,10] Marek Jurek,[9] Ryszard Sobierajski,[9] Jacek Krzywinski,[11] Stefan Moeller,[11] Marion Harmand,[6,12] Germano Galasso,[13] Mitsuru Nagasono,[14] Karel Saskl,[15] Pavol Sovák,[16] and Libor Juha[1]

[1]*Institute of Physics, Academy of Sciences of the Czech Republic, Na Slovance 2, Prague 8, 182 21, Czech Republic*
[2]*Faculty of Mathematics and Physics, Charles University in Prague, V Holesovickach 2, Praha 8, 180 00, Czech Republic*
[3]*Paul Scherrer Institut, 5232 Villigen PSI, Switzerland*
[4]*European XFEL GmbH, Albert-Einstein-Ring 19, Hamburg, D-22671, Germany*
[5]*CELIA, Uni. Bordeaux, CEA, CNRS 351, Cours de la Libération, F-33405 Talence cedex, France*
[6]*Photon Science, DESY, Notkestr. 85, Hamburg D-22607, Germany*
[7]*Center for Free-Electron Laser Science, Notkestr. 85, Hamburg, D-22607, Germany*
[8]*Department of Physics, University of Hamburg, Luruper Chaussee 149, Hamburg, D-22761, Germany*
[9]*Institute of Physics, Polish Academy of Sciences, Al. Lotników 32/46, Warsaw, PL-02-668, Poland*
[10]*FOM Institute DIFFER, Nieuwegein, The Netherlands*
[11]*SLAC National Accelerator Laboratory, 2575 Sand Hill Road, Menlo Park, California 94025, USA*
[12]*Institut de minéralogie, de physique des matériaux et de cosmochimie, Unité mixte de recherche (CNRS, UPMC, MNHN et IRD), 4 place Jussieu, 75005, Paris, France*
[13] *Institut für Mechanik und Mechatronik, Technische Universität Wien, Wiedner Hauptstraße 8-10, Wien, Austria*
[14]*RIKEN/SPring-8 Kouto 1-1-1, Sayo, Hyogo, 679-5148 Japan*
[15]*Institute of Materials Research, Slovak Academy of Sciences, Kosice, 040 01, Slovak Republic*
[16]*Institute of Physics, P. J. Šafárik University, Park Angelinum, Kosice, 04154, Slovak Republic*
[*]*burian@fzu.cz*

Abstract: An irreversible response of inorganic scintillators to intense soft x-ray laser radiation was investigated at the FLASH (Free-electron LASer in Hamburg) facility. Three ionic crystals, namely, Ce:YAG (cerium-doped yttrium aluminum garnet), $PbWO_4$ (lead tungstate), and ZnO (zinc oxide), were exposed to single 4.6 nm ultra-short laser pulses of variable pulse energy (up to 12 μJ) under normal incidence conditions with tight focus. Damaged areas produced with various levels of pulse fluences, were analyzed on the surface of irradiated samples using differential interference contrast (DIC) and atomic force microscopy (AFM). The effective beam area of 22.2 ± 2.2 μm^2 was determined by means of the ablation imprints method with the use of poly(methyl methacrylate) - PMMA. Applied to the three inorganic materials, this procedure gave almost the same values of an effective area. The single-shot damage threshold fluence was determined for each of these inorganic materials. The Ce:YAG sample seems to be the most radiation resistant under the given irradiation conditions, its damage threshold was determined to be as high as 660.8 ± 71.2 mJ/cm^2. Contrary to that, the $PbWO_4$ sample exhibited the lowest radiation resistance with a threshold fluence of 62.6 ± 11.9 mJ/cm^2. The threshold for ZnO was found to be 167.8 ± 30.8 mJ/cm^2. Both interaction and material characteristics responsible for the damage threshold difference are discussed in the article.

OCIS codes: (160.2540) Fluorescent and luminescent materials; (140.3330) Laser damage; (140.2600) Free-electron lasers (FELs); (260.6048) Soft x-rays; (350.3390) Laser materials processing.

References and links

1. D. Attwood, *Soft X-Rays and Extreme Ultraviolet Radiation: Principles and Applications* (Cambridge University Press, Cambridge, 1999).

#224407 - $15.00 USD Received 9 Oct 2014; revised 15 Dec 2014; accepted 17 Dec 2014; published 7 Jan 2015

2. P. Jaeglé, *Coherent Sources of XUV Radiation: Soft X-Ray Lasers and High-Order Harmonic Generation* (Springer, 2006).
3. E. L. Saldin, E. A. Schneidmiller, and M. E. Yurkov, *The Physics of Free-Electron Lasers* (Springer-Verlag, 2000).
4. P. Schmüser, M. Dohlus, J. Rossbach, and C. Behrens, *Free-Electron Lasers in the Ultraviolet and X-ray Regime*, 2nd ed. (Springer-Verlag, 2014).
5. M. Nikl, "Scintillation detectors for X-rays," Meas. Sci. Technol. **17**(4), R37–R54 (2006).
6. A. A. Annenkov, M. V. Korzik, and P. Lecoq, "Lead tungstate scintillation material," Nucl. Instrum. Methods Phys. Res. A **490**(1-2), 30–50 (2002).
7. T. Shimizu, K. Yamanoi, K. Sakai, M. Cadatal-Raduban, T. Nakazato, N. Sarukura, M. Kano, A. Wakamiya, D. Ehrentraut, T. Fukuda, M. Nagasono, T. Togashi, S. Matsubara, K. Tono, A. Higashiya, M. Yabashi, H. Kimura, H. Ohashi, and T. Ishikawa, "Response time-shortened zinc oxide scintillator for accurate single-shot synchronization of extreme ultraviolet free-electron laser and short-pulse laser," Appl. Phys. Express **4**(6), 062701 (2011).
8. M. Kirm, A. Andrejczuk, J. Krzywinski, and R. Sobierajski, "Influence of excitation density on luminescence decay in $Y_3Al_5O_{12}$:Ce and BaF_2 crystals excited by free electron laser radiation in VUV," Phys. Status Solidi **2**(1 c), 649–652 (2005).
9. D. P. Bernstein, Y. Acremann, A. Scherz, M. Burkhardt, J. Stöhr, M. Beye, W. F. Schlotter, T. Beeck, F. Sorgenfrei, A. Pietzsch, W. Wurth, and A. Föhlisch, "Near edge x-ray absorption fine structure spectroscopy with x-ray free electron lasers," Appl. Phys. Lett. **95**(13), 134102 (2009).
10. M. Nikl, E. Mihokova, V. Laguta, J. Pejchal, S. Baccaro, and A. Vedda, "Radiation damage processes in complex-oxide scintillators," Proc. SPIE **6586**, 65860E (2007).
11. V. Ayvazyan, N. Baboi, J. Bähr, V. Balandin, B. Beutner, A. Brandt, I. Bohnet, A. Bolzmann, R. Brinkmann, O. I. Brovko, J. P. Carneiro, S. Casalbuoni, M. Castellano, P. Castro, L. Catani, E. Chiadroni, S. Choroba, A. Cianchi, H. Delsim-Hashemi, G. Di Pirro, M. Dohlus, S. Düsterer, H. T. Edwards, B. Faatz, A. A. Fateev, J. Feldhaus, K. Flöttmann, J. Frisch, L. Fröhlich, T. Garvey, U. Gensch, N. Golubeva, H.-J. Grabosch, B. Grigoryan, O. Grimm, U. Hahn, J. H. Han, M. V. Hartrott, K. Honkavaara, M. Hüning, R. Ischebeck, E. Jaeschke, M. Jablonka, R. Kammering, V. Katalev, B. Keitel, S. Khodyachykh, Y. Kim, V. Kocharyan, M. Körfer, M. Kollewe, D. Kostin, D. Krämer, M. Krassilnikov, G. Kube, L. Lilje, T. Limberg, D. Lipka, F. Löhl, M. Luong, C. Magne, J. Menzel, P. Michelato, V. Miltchev, M. Minty, W. D. Möller, L. Monaco, W. Müller, M. Nagl, O. Napoly, P. Nicolosi, D. Nölle, T. Nuñez, A. Oppelt, C. Pagani, R. Paparella, B. Petersen, B. Petrosyan, J. Pflüger, P. Piot, E. Plönjes, L. Poletto, D. Proch, D. Pugachov, K. Rehlich, D. Richter, S. Riemann, M. Ross, J. Rossbach, M. Sachwitz, E. L. Saldin, W. Sandner, H. Schlarb, B. Schmidt, M. Schmitz, P. Schmüser, J. R. Schneider, E. A. Schneidmiller, H.-J. Schreiber, S. Schreiber, A. V. Shabunov, D. Sertore, S. Setzer, S. Simrock, E. Sombrowski, L. Staykov, B. Steffen, F. Stephan, F. Stulle, K. P. Sytchev, H. Thom, K. Tiedtke, M. Tischer, R. Treusch, D. Trines, I. Tsakov, A. Vardanyan, R. Wanzenberg, T. Weiland, H. Weise, M. Wendt, I. Will, A. Winter, K. Wittenburg, M. V. Yurkov, I. Zagorodnov, P. Zambolin, and K. Zapfe, "First operation of a free-electron laser generating GW power radiation at 32 nm wavelength," Eur. Phys. J. D **37**(2), 297–303 (2006).
12. P. Emma, R. Akre, J. Arthur, R. Bionta, C. Bostedt, J. Bozek, A. Brachmann, P. Bucksbaum, R. Coffee, F.-J. Decker, Y. Ding, D. Dowell, S. Edstrom, A. Fisher, J. Frisch, S. Gilevich, J. Hastings, G. Hays, Ph. Hering, Z. Huang, R. Iverson, H. Loos, M. Messerschmidt, A. Miahnahri, S. Moeller, H.-D. Nuhn, G. Pile, D. Ratner, J. Rzepiela, D. Schultz, T. Smith, P. Stefan, H. Tompkins, J. Turner, J. Welch, W. White, J. Wu, G. Yocky, and J. Galayda, "First lasing and operation of an ångstrom-wavelength free-electron laser," Nat. Photonics **4**(9), 641–647 (2010).
13. T. Ishikawa, H. Aoyagi, T. Asaka, Y. Asano, N. Azumi, T. Bizen, H. Ego, K. Fukami, T. Fukui, Y. Furukawa, S. Goto, H. Hanaki, T. Hara, T. Hasegawa, T. Hatsui, A. Higashiya, T. Hirono, N. Hosoda, M. Ishii, T. Inagaki, Y. Inubushi, T. Itoga, Y. Joti, M. Kago, T. Kameshima, H. Kimura, Y. Kirihara, A. Kiyomichi, T. Kobayashi, C. Kondo, T. Kudo, H. Maesaka, X. M. Maréchal, T. Masuda, S. Matsubara, T. Matsumoto, T. Matsushita, S. Matsui, M. Nagasono, N. Nariyama, H. Ohashi, T. Ohata, T. Ohshima, S. Ono, Y. Otake, Ch. Saji, T. Sakurai, T. Sato, K. Sawada, T. Seike, K. Shirasawa, T. Sugimoto, S. Suzuki, S. Takahashi, H. Takebe, K. Takeshita, K. Tamasaku, H. Tanaka, R. Tanaka, T. Tanaka, T. Togashi, K. Togawa, A. Tokuhisa, H. Tomizawa, K. Tono, S. Wu, M. Yabashi, M. Yamaga, A. Yamashita, K. Yanagida, Ch. Zhang, T. Shintake, H. Kitamura, and N. Kumagai, "A compact X-ray free-electron laser emitting in the sub-ångström region," Nat. Photonics **6**(8), 540–544 (2012).
14. E. Allaria, R. Appio, L. Badano, W. A. Barletta, S. Bassanese, S. G. Biedron, A. Borga, E. Busetto, D. Castronovo, P. Cinquegrana, S. Cleva, D. Cocco, M. Cornacchia, P. Craievich, I. Cudin, G. D'Auria, M. Dal Forno, M. B. Danailov, R. De Monte, G. De Ninno, P. Delgiusto, A. Demidovich, S. Di Mitri, B. Diviacco, A. Fabris, R. Fabris, W. Fawley, M. Ferianis, E. Ferrari, S. Ferry, L. Froehlich, P. Furlan, G. Gaio, F. Gelmetti, L. Giannessi, M. Giannini, R. Gobessi, R. Ivanov, E. Karantzoulis, M. Lonza, A. Lutman, B. Mahieu, M. Milloch, S. V. Milton, M. Musardo, I. Nikolov, S. Noe, F. Parmigiani, G. Penco, M. Petronio, L. Pivetta, M. Predonzani, F. Rossi, L. Rumiz, A. Salom, C. Scafuri, C. Serpico, P. Sigalotti, S. Spampinati, C. Spezzani, M. Svandrlik, C. Svetina, S. Tazzari, M. Trovo, R. Umer, A. Vascotto, M. Veronese, R. Visintini, M. Zaccaria, D. Zangrando, and M. Zangrando, "Highly coherent and stable pulses from the FERMI seeded free-electron laser in the extreme ultraviolet," Nat. Photonics **6**(10), 699–704 (2012).

#224407 - $15.00 USD Received 9 Oct 2014; revised 15 Dec 2014; accepted 17 Dec 2014; published 7 Jan 2015

15. N. Itoh and A. M. Stoneham, *Materials Modification by Electronic Excitation* (Cambridge University Press, Cambridge, 2001) and references cited therein.
16. P. Bohacek, M. Nikl, J. Novak, Z. Malkova, B. Trunda, J. Rysavy, S. Baccaro, A. Cecilia, I. Dafinei, M. Diemoz, and K. Jurek, "Congruent composition of $PbWO_4$ single crystals," J. Electrical Eng. **50**, 38–40 (1999).
17. J. Kvapil, J. Kvapil, B. Manek, B. Perner, R. Autrata, and P. Schauer, "Czochralski growth of YAG:Ce in a reducing protective atmosphere," J. Cryst. Growth **52**, 542–545 (1981).
18. K. Tiedtke, A. Azima, N. von Bargen, L. Bittner, S. Bonfigt, S. Düsterer, B. Faatz, U. Frühling, M. Gensch, Ch. Gerth, N. Guerassimova, U. Hahn, T. Hans, M. Hesse, K. Honkavaar, U. Jastrow, P. Juranic, S. Kapitzki, B. Keitel, T. Kracht, M. Kuhlmann, W. B. Li, M. Martins, T. Núñez, E. Plönjes, H. Redlin, E. L. Saldin, E. A. Schneidmiller, J. R. Schneider, S. Schreiber, N. Stojanovic, F. Tavella, S. Toleikis, R. Treusch, H. Weigelt, M. Wellhöfer, H. Wabnitz, M. V. Yurkov, and J. Feldhaus, "The soft x-ray free-electron laser FLASH at DESY: beamlines, diagnostics and end-stations," New J. Phys. **11**(2), 023029 (2009).
19. R. Sobierajski, M. Jurek, J. Chalupský, J. Krzywinski, T. Burian, S. D. Farahani, V. Hájková, M. Harmand, L. Juha, D. Klinger, R. A. Loch, C. Ozkan, J. B. Pełka, K. Sokolowski-Tinten, H. Sinn, S. Toleikis, K. Tiedtke, T. Tschentscher, H. Wabnitz, and J. Gaudin, "Experimental set-up and procedures for the investigation of XUV free electron laser interactions with solids," J. Instrum. **8**, P02010 (2013).
20. B. L. Henke, E. M. Gullikson, and J. C. Davis, "X-ray interactions - photoabsorption, scattering, transmission, and reflection at E=50-30,000 eV, Z=1-92," Atom. Data Nucl. Data **54**, 181–342 (1993); http://henke.lbl.gov/optical_constants/
21. M. Richter, A. Gottwald, U. Kroth, A. A. Sorokin, S. V. Bobashev, L. A. Shmaenok, J. Feldhaus, Ch. Gerth, B. Steeg, K. Tiedtke, and R. Treusch, "Measurement of gigawatt radiation pulses from a vacuum and extreme ultraviolet free-electron laser," Appl. Phys. Lett. **83**(14), 2970–2972 (2003).
22. J. Chalupský, J. Krzywinski, L. Juha, V. Hájková, J. Cihelka, T. Burian, L. Vysín, J. Gaudin, A. Gleeson, M. Jurek, A. R. Khorsand, D. Klinger, H. Wabnitz, R. Sobierajski, M. Störmer, K. Tiedtke, and S. Toleikis, "Spot size characterization of focused non-Gaussian X-ray laser beams," Opt. Express **18**(26), 27836–27845 (2010).
23. J. Chalupský, T. Burian, V. Hájková, L. Juha, T. Polcar, J. Gaudin, M. Nagasono, R. Sobierajski, M. Yabashi, and J. Krzywinski, "Fluence scan: an unexplored property of a laser beam," Opt. Express **21**(22), 26363–26375 (2013).
24. J. Krzywinski, R. Sobierajski, M. Jurek, R. Nietubyc, J. B. Pelka, L. Juha, M. Bittner, V. Létal, V. Vorlíček, A. Andrejczuk, J. Feldhaus, B. Keitel, E. L. Saldin, E. A. Schneidmiller, R. Treusch, and M. V. Yurkov, "Conductors, semiconductors, and insulators irradiated with short-wavelength free-electron laser," J. Appl. Phys. **101**(4), 043107 (2007).
25. J. Chalupský, L. Juha, J. Kuba, J. Cihelka, V. Hájková, S. Koptyaev, J. Krása, A. Velyhan, M. Bergh, C. Caleman, J. Hajdu, R. M. Bionta, H. Chapman, S. P. Hau-Riege, R. A. London, M. Jurek, J. Krzywinski, R. Nietubyc, J. B. Pelka, R. Sobierajski, J. Meyer-Ter-Vehn, A. Tronnier, K. Sokolowski-Tinten, N. Stojanovic, K. Tiedtke, S. Toleikis, T. Tschentscher, H. Wabnitz, and U. Zastrau, "Characteristics of focused soft X-ray free-electron laser beam determined by ablation of organic molecular solids," Opt. Express **15**(10), 6036–6043 (2007).
26. L. R. Holland, G. M. Jenkins, J. H. Fisher, W. A. Hollerman, and G. A. Shelby, "Efficiency and radiation hardness of phosphors in a proton beam," Nucl. Instrum. Methods Phys. Res. B **56–57**, 1239–1241 (1991).
27. M. Nikl, K. Nitsch, S. Baccaro, A. Cecilia, M. Montecchi, B. Borgia, I. Dafinei, M. Diemoz, M. Martini, E. Rosetta, G. Spinolo, A. Vedda, M. Kobayashi, M. Ishii, Y. Usuki, O. Jarolimek, and P. Reiche, "Radiation induced formation of color centers in $PbWO_4$ single crystals," J. Appl. Phys. **82**(11), 5758–5762 (1997).
28. R. Y. Zhu, "Radiation damage in scintillating crystals," Nucl. Instrum. Methods Phys. Res. A **413**(2-3), 297–311 (1998).
29. P. Kozma and P. Kozma, Jr., "Radiation resistance of heavy scintillators to low-energy gamma-rays," Radiat. Phys. Chem. **71**(3-4), 705–707 (2004).
30. G. Pari, A. Mookerjeee, and A. K. Bhattacharya, "Study of α-Al_2O_3 and the role of Y in $YAlO_3$ and $Y_3Al_5O_{12}$ by first principles electronic structure calculations," Condens. Matter Phys. **36**, 36057921 (2004).
31. P. Erhart, N. Juslin, O. Goy, K. Nordlund, R. Müller, and K. Albe, "Analytic bond-order potential for atomistic simulations of zinc oxide," J. Phys. Condens. Matter **18**(29), 6585–6605 (2006).
32. N. Medvedev and B. Rethfeld, "Effective energy gap of semiconductors under irradiation with an ultrashort VUV laser pulse," Europhys. Lett. **88**(5), 55001 (2009).
33. A. F. G. Leontowich, A. Aquila, F. Stellato, R. Bean, H. Fleckenstein, M. Prasciolu, M. Liang, D. P. DePonte, A. Barty, F. Wang, J. Andreasson, J. Hajdu, H. N. Chapman, and S. Bajt, "Characterizing the focus of a multilayer coated off-axis parabola for FLASH beam at $\lambda = 4.3$ nm," Proc. of SPIE 8777, 87770T–1 (2013).

1. Introduction

Scintillators play an important role in short-wavelength radiation research with respect to development, characterization, and utilization of sources generating intense radiation in the extreme ultraviolet and soft x-ray spectral regions. For more than a century, it is known that some materials are capable of converting energy of photons or particles into visible light or ultraviolet radiation that can be easily detected. The advent of CCDs made the imaging of

#224407 - $15.00 USD Received 9 Oct 2014; revised 15 Dec 2014; accepted 17 Dec 2014; published 7 Jan 2015

such converted radiation easy and inexpensive. Scintillators greatly simplify the procedure of detection and visualization of otherwise invisible radiation, enabling easier and faster tracing and alignment of short-wavelength beams provided mostly by free-electron lasers and synchrotron radiation sources.

The rapid development of new extreme ultraviolet and soft x-ray lasers during the last two decades [1–4] has opened new possibilities in research of the interaction of short-wavelength radiation with matter. However, this also raises new challenges for the applicability of scintillator materials. The scintillator properties required for short-wavelength laser beam characterization and imaging are as follows: a high yield of luminescence, a well-defined dependence of the yield on radiation properties (e.g., well-known dependence of the yield as a function of radiation intensity) fast response to the ultra-short laser pulses, sufficiently high absorption coefficient and damage threshold. For example, $PbWO_4$ [5,6] or ZnO [7] single crystals, with decay times of 2-3 ns and less than 1 ns (down to a few picoseconds dependent on doping concentration), respectively, can be used for detecting, timing and imaging short and ultra-short pulses of x-ray lasers [1–4]. The third material chosen for our experiment, Ce:YAG (Ce:$Y_3Al_5O_{12}$) crystal, is widely used for the soft X-ray laser beam imaging and characterization because of its high luminescent yield and excellent radiation resistance [8–10].

Radiation resistance of scintillating crystals has to be considered when being used as short-wavelength radiation monitors, in order to prevent irreversible changes of their crystal structure or even damage. This follows from the fact that currently available free-electron lasers (FELs) generate 10-fs – 100-fs pulses, each carrying an energy equal to hundreds of microjoules [11–14]. The peak intensity in focused FEL beams can reach levels above 10^{17} W/cm^2 while the peak fluence can exceed kJ/cm^2. Therefore, irradiation conditions resulting in a collapse of the crystal lattice in the scintillation material can be achieved even for weakly focused FEL beams.

Even at intensities many orders of magnitude lower than the above mentioned value, e.g. in an unfocused FEL beam, the scintillators are operated far beyond the linear regime and thus non-linear intensity-dependent response (mostly saturation) of the luminescence signal can be observed [8,9]. At higher intensities, irreversible chemical and structural changes occur on the surface and in the near-surface layer of the material exposed to FEL radiation. Hence, exact knowledge of the threshold fluence, i.e., a minimum fluence resulting in a detectable irreversible modification of the irradiated material surface, is required for safe usage of scintillators at large-scale FEL facilities.

The above-mentioned FEL-induced substantial (i.e., from a phase transition to a removal of irradiated material) damage differs from the radiation damage as usually taken into account for a scintillator exposed to a common ionizing radiation. In the scintillator community, the radiation damage is defined as a formation of radio-luminescence yield influencing point defects and their small complexes (clusters) in the lattice, see for example [15]. We are aware that a radiation resistance of the whole lattice against its substantial collapse is more complex and still poorly understood phenomenon. Here we assume that a certain lattice, yielding effectively point defects under conventional irradiation conditions (i.e., color centers formation, production of defects enhancing non-radiative recombination of charge carriers, and so on), could be more prone to a substantial lattice collapse upon the FEL-irradiation. It is understood this picture represents only a first approximation.

2. Experimental

Single crystals of $PbWO_4$ and Ce:YAG were grown from high-temperature melt of the corresponding material using the Czochralski technique [16,17] while monocrystalline ZnO was prepared by a conventional hydro-thermal technique [7].

The experiment was performed at the free electron laser facility FLASH (Free-electron LASer in Hamburg) [11,18]. Samples were mounted on a motorized X-Y-Z stage inside a

#224407 - $15.00 USD Received 9 Oct 2014; revised 15 Dec 2014; accepted 17 Dec 2014; published 7 Jan 2015

vacuum chamber [19] and exposed to focused single pulses. Pulse duration fluctuated between 80 fs and 150 fs. Beamline optics involved three amorphous carbon (a-C) coated mirrors and two Ni coated mirrors with grazing angles adjusted to 3° and 2°, respectively. In order to prevent the a-C coated mirrors from radiation damage and avoid unwanted reflectivity losses, the laser was tuned on the long-wavelength side of the carbon K-edge (4.37 nm). The laser wavelength was measured as 4.6 ± 0.1 nm. A total beamline transmission of this experimental layout was assumed to be 0.39, as calculated using CXRO database [20] and taking into account the reflectivity at 4.6 nm of all optical elements in the beamline.

Energy in each laser shot was monitored with a photo-ionizing gas detector (GMD – Gas Monitor Detector) [18,21]. To adjust the desired fluence level impinging on the sample, the laser beam was attenuated with a gas attenuator in combination with a set of thin aluminium foils of various thicknesses.

Irradiated samples were inspected and damage patterns were investigated ex-situ using an optical microscope (Olympus BX51M) operated in differential interference contrast (DIC) mode and Dimension 3100 scanning probe microscope (SPM) driven by a NanoScope IV controller (Veeco, USA) working in AFM tapping mode.

3. Results and discussion

Since the damage threshold fluence is defined as:

$$F_{th} = \frac{E_{th}}{A_{eff}} \tag{1}$$

where F_{th} [J/cm^2], E_{th} [J], and A_{eff} [cm^2] represent the threshold fluence, threshold pulse energy, and effective area of the beam in the plane of the sample surface, respectively, the knowledge of the beam size is indispensable for the process of threshold fluence determination. In order to attain this value, a method of ablative imprints on the surface of a PMMA sample [22] was used. 5 μm thick layer of PMMA spin coated onto a silicon slab was used for focused beam size determination. Sequences of single laser shots at various energy levels were imprinted onto the surface of this sample. The dependence of the damaged area on the logarithm of the corresponding pulse energy (the so called Liu's plot) is shown in Fig. 1(a). Non-linearity of the Liu's plot clearly indicates that the beam was non-Gaussian; therefore, only the low-energy part of the plot is used for the linear fit of the data. By extrapolating the linear part of the data to zero imprint area, where no damage occurs, thus finding out the intersection of the regression line with the horizontal axis, one obtains the threshold pulse energy of E_{th} = (55.5 ± 5.3) nJ.

The ratio between the threshold energy E_{th} and laser pulse energy E_{pulse}, i.e. the threshold-to-peak ratio $f = E_{th}/E_{pulse}$, was plotted against the area S circumscribed on the sample surface by ablation contour (a borderline between the damaged and morphologically unperturbed sample surfaces) as shown in Fig. 1(b). Such a plot is also known as the normalized f-scan (fluence scan) [23]. The area being enveloped by the f-scan curve is equal to the effective beam area. In order to measure it, data in Fig. 1(b) were fitted with a normalized sum of two exponential functions:

$$f(S) = A \cdot e^{-C_1 S} + (1 - A) \cdot e^{-C_2 S} \tag{2}$$

where A, C_1, and C_2 are parameters of the fit. The fitting function in Eq. (2) approximates the real beam as an incoherent superposition of two Gaussian beams with effective areas $1/C_1$ and $1/C_2$. The transverse fluence distribution in the studied laser beam is thus presumed to have a narrow central peak being surrounded by broadened background (wings). As mentioned above the effective area of the laser beam A_{eff} can be calculated as follows:

#224407 - $15.00 USD Received 9 Oct 2014; revised 15 Dec 2014; accepted 17 Dec 2014; published 7 Jan 2015

$$A_{eff} = \int_0^{\infty} \left\{ A \cdot e^{-C_1 S} + (1-A) \cdot e^{-C_2 S} \right\} dS = \frac{A}{C_1} + \frac{1-A}{C_2} \qquad (3)$$

Evaluating Eq. (3) for the fit of the PMMA data gives us the effective beam area of 22.2 ± 2.2 μm^2. Using Eq. (1) we calculate that the threshold fluence of PMMA, present at 4.6 nm wavelength, is as high as 250 ± 34.4 mJ/cm^2.

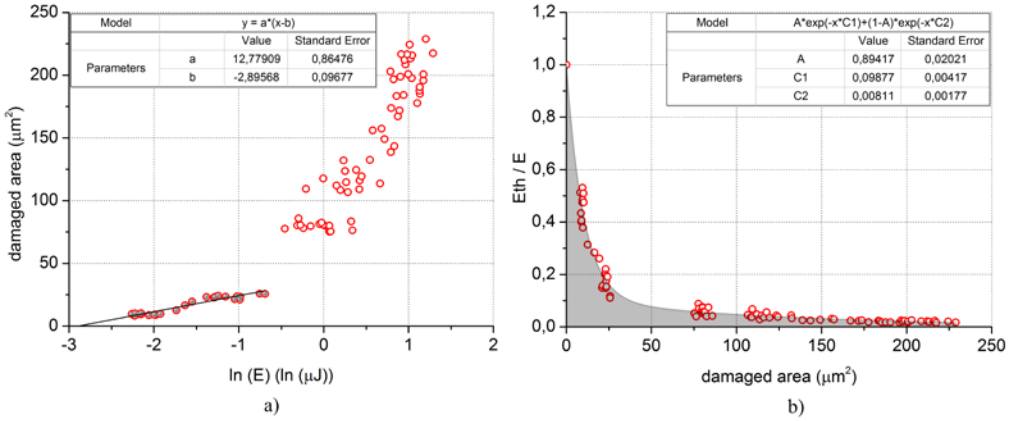

Fig. 1. (a) Liu's plot of damaged areas on the PMMA surface determines the threshold energy for the ablation process. Only the linear part of the plot (grey-filled data points) is taken into account for the purposes of the threshold energy extrapolation. (b) Area under the fitting curve in the normalized f-scan provides information about the effective beam area.

The same procedure, as in the case of PMMA, was applied to inorganic scintillators. Microscopy images of damaged areas on the $PbWO_4$ surface eroded at high (a) and low (b) FLASH fluence are compared in Fig. 2. The edges of the craters do not exhibit any crack or other sign of a thermo-mechanical damage, and/or spur of expanded molten material. Such a clean ablation was observed in all the ionic crystals investigated in the presented study.

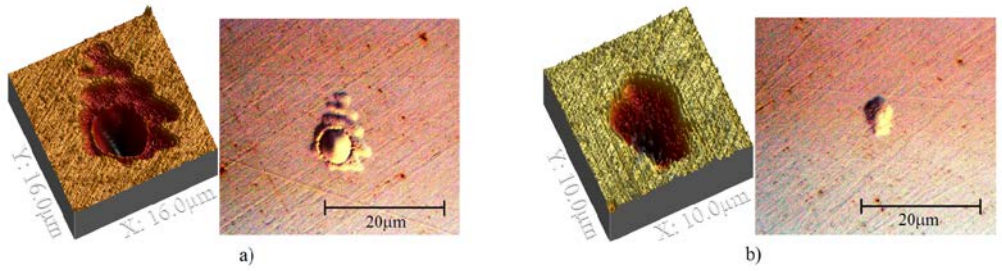

Fig. 2. Comparison of morphology of craters eroded in the $PbWO_4$ sample at a fluence of (a) 35-fold and (b) 4-fold above the single-shot ablation threshold, as taken with AFM (left) and DIC (right) microscope.

From the Liu's plots the threshold energies were determined and their values were used to evaluate threshold fluences of the investigated materials. The effective area of the beam was assumed to be the same as in the case of PMMA. However, for the purposes of comparison, the effective beam area was independently evaluated from the data obtained with the scintillator crystals. All the data and results are summarized in Figs. 3(a) and 3(b) (for Ce:YAG), Figs. 4(a) and 4(b) (for $PbWO_4$), Figs. 5(a) and 5(b) (for ZnO), and Table 1 (for all FLASH-irradiated materials).

#224407 - $15.00 USD Received 9 Oct 2014; revised 15 Dec 2014; accepted 17 Dec 2014; published 7 Jan 2015

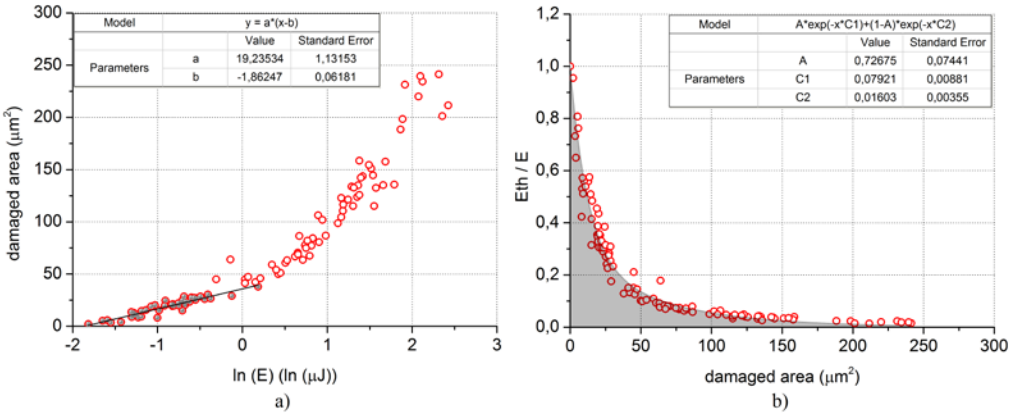

Fig. 3. (a) Liu's plot for Ce:YAG with determined threshold energy and (b) the corresponding normalized f-scan.

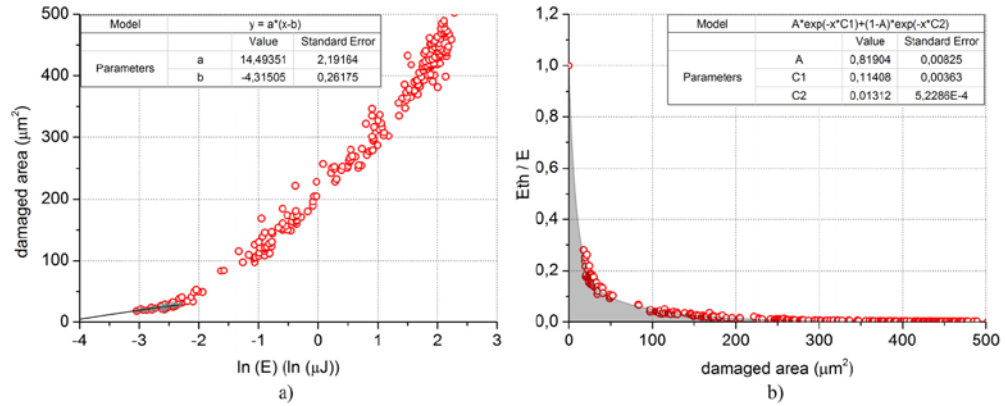

Fig. 4. (a) Liu's plot for $PbWO_4$ with determined threshold energy and (b) the corresponding normalized f-scan.

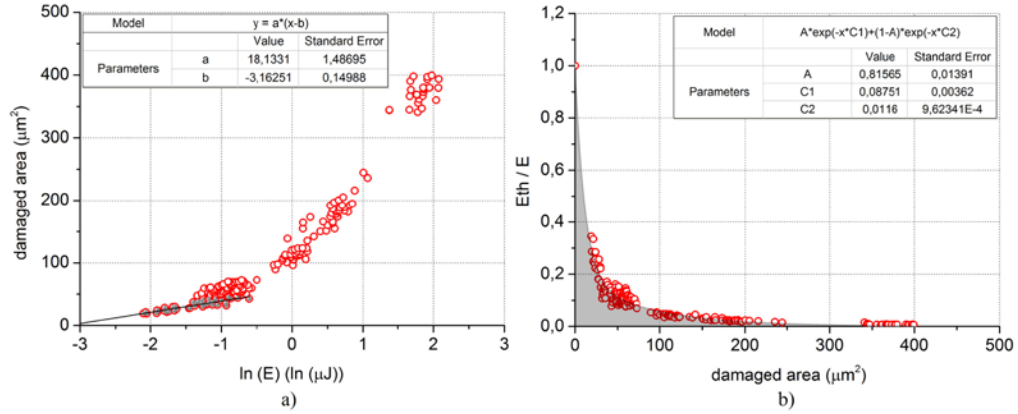

Fig. 5. (a) Liu's plot for ZnO with determined threshold energy and (b) the corresponding normalized f-scan.

#224407 - $15.00 USD Received 9 Oct 2014; revised 15 Dec 2014; accepted 17 Dec 2014; published 7 Jan 2015

Table 1. Summary of key characteristics of the selected materials irradiated by 4.6 nm FLASH radiation

Material	Threshold energy [nJ]	Effective area [μm^2]	Threshold fluence [mJ/cm^2]
PMMA	55.5 ± 5.3	22.2 ± 2.2	250 ± 34.4
Ce:YAG	155.3 ± 3.8	23.5 ± 4.8	660.8 ± 71.2
$PbWO_4$	13.4 ± 2.3	21.4 ± 4.6	62.6 ± 11.9
ZnO	42.3 ± 5.4	25.2 ± 6.3	167.8 ± 30.8

Values of the threshold fluences were calculated from Eq. (1), taking into account the effective area obtained from PMMA.

The Ce:YAG sample seems to be the most radiation-resistant at this wavelength with the damage threshold as high as 660.8 ± 71.2 mJ/cm^2. The $PbWO_4$ sample exhibited the lowest radiation resistance with the threshold fluence of only 62.6 ± 11.9 mJ/cm^2. The threshold for ZnO was found to be 167.8 ± 30.8 mJ/cm^2. The value for Ce:YAG is much higher than the previously reported damage threshold result of about 20 mJ/cm^2 [24]. However, our value was obtained for irradiation with 4.6 nm wavelength FEL beam while previous results were obtained for the extreme ultraviolet (89 nm) FEL radiation. This difference is most likely due to a significantly shorter absorption length of extreme ultraviolet radiation as compared to soft X-rays, i.e. absorption lengths of 17.8 nm and 95.8 nm [20], respectively. Therefore, at the same fluence we obtain much greater energy density in the near surface layer of the sample with the laser operating in the extreme ultraviolet spectral range

We also take into account that the radiation hardness reported here, in terms of the threshold fluence, is influenced by two key factors: the intrinsic radiation resistance of the crystal lattice to an energetic photon and, an attenuation length controlled term showing how strongly the FEL radiation is absorbed in the particular material. The value of an attenuation length can be easily extracted as a slope, with a linear fit, in the low energy part of the dependence of maximal crater depth on the logarithm of pulse energy [25], as shown in Fig. 6.

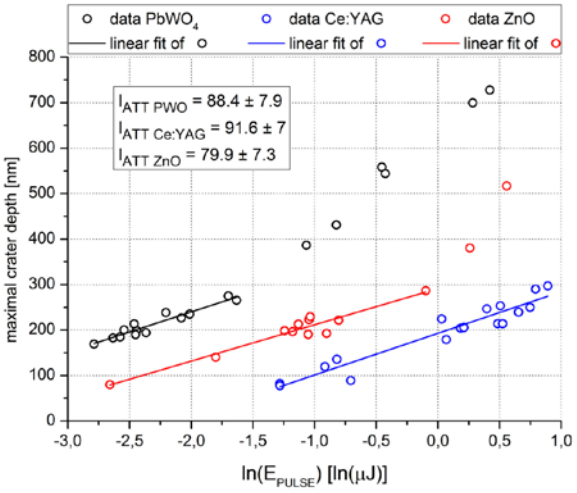

Fig. 6. Dependence of maximal crater depth on the logarithm of pulse energy. The slopes of fits are equal to the attenuation lengths in the irradiated material.

We can also estimate a critical energy dose D_C *[J/mm^3]* related to the investigated material under given irradiation conditions as follows:

#224407 - $15.00 USD Received 9 Oct 2014; revised 15 Dec 2014; accepted 17 Dec 2014; published 7 Jan 2015

$$D_C = \frac{F_{th}}{l_{att}} \quad (4)$$

All attenuation lengths and critical doses for investigated materials are summarized in Table 2. With a value of 2470 nm determined according to the Henke's Tables [20], PMMA's attenuation length is more than twenty times higher than scintillators investigated until now. Although intrinsic radiation resistance of any organic polymer is much lower than the radiation stability of inorganic materials reported here, the significantly longer attenuation length in PMMA, places PMMA's threshold above the threshold of $PbWO_4$. The most surprising finding (see Table 2) is that the radiation damage threshold in $PbWO_4$ is significantly lower than in Ce:YAG. Since the attenuation lengths are almost the same in both materials, the difference in thresholds could be caused by higher intrinsic radiation resistance of Ce:YAG to 4.6 nm radiation as compared to $PbWO_4$. Both Ce:YAG and $PbWO_4$ are recognized in the literature as radiation hard materials [6,10,26–29] but our results show that Ce:YAG exhibits much higher intrinsic radiation stability than $PbWO_4$. When comparing our values with scintillator radiation hardness reported in the literature, we have to take into account that the previous reports [6,10,26–29] are mainly dealing with the formation of radiation defects (mostly color centers and other point defects) of the lattice and not with a substantial decomposition of the lattice (as caused by FLASH radiation above a single-shot damage threshold fluence).

Experimentally determined critical doses (Table 2) are in all three cases higher than energy densities needed for thermal melting of the material, calculated from values of specific heat capacities, melting points and latent heats of melting found in the literature for a particular material investigated here. This indicates that material ablation (i.e., the material in sample regions irradiated above the ablation threshold is not only molten, but completely transferred into the vacuum) is the key process responsible for the damage in all three investigated inorganic materials irradiated by 4.6 nm FEL radiation. However, the observed critical density values are lower than the values needed for overcoming cohesive energies reported for corresponding crystals in the literature [30,31]. Lowering of the energy required for substantial lattice decomposition could be explained by an effect of electronic excitation and internal ionization in the ablation process driven by the soft X-ray laser. Additional support for this explanation is the fact that Ce:YAG, which has the highest stability under the irradiation conditions, also has the widest band gap (>7eV) among the three ionic crystals investigated. Although the theory of the role of the gap in insulators is not developed as much as for semiconductors [32], we assume that a wider gap reduces the number and the energy of electrons transferred from the valence band of the irradiated ionic crystal to its conduction band. The fraction of the transferred electrons seems to be critical for the non-thermal collapse of the lattice.

Table 2. Comparison of tabulated attenuation lengths (taken from CXRO tables) with values obtained from experimental ablation data.

Material	Attenuation length - from CXRO tables [nm]	Attenuation length - from experiment [nm]	Critical energy density - from experiment [J/mm^3]	Critical energy density - from melting [J/mm^3]	Critical energy density - from cohesive energy [J/mm^3]
Ce:YAG	95.8	91.6 ± 7	72.1 ± 9.5	8.4	121.7
$PbWO_4$	92.6	88.4 ± 7.9	7.1 ± 1.5	4.1	-----
ZnO	80	79.9 ± 7.3	21 ± 4.3	6.7	43.3

An effective FEL-beam area on a particular material and an experimental value of an attenuation length were used for evaluating the critical energy density (critical dose) of 4.6 nm radiation. Experimentally determined critical doses can be compared to a critical energy density required for thermal melting of a particular material and for the substantial decomposition of the lattice by its evaporation derived from a cohesive energy of a particular crystal. A cohesive energy of $PbWO_4$ is not yet reported in the literature.

#224407 - $15.00 USD Received 9 Oct 2014; revised 15 Dec 2014; accepted 17 Dec 2014; published 7 Jan 2015

Evaluation of the threshold pulse energy is difficult, especially if a low radiation resistant material is used. In order to cross the threshold energy, the beam has to be strongly attenuated, which increases the uncertainty in the energy measurement significantly. In the worst case the required attenuation level cannot be reached at all. The latter case applies to the PMMA, ZnO, and $PbWO_4$ as seen in Liu's plots (Figs. 3(a), 4(a), 5(a)). Even for the highest attenuation the energy deposited on the samples is well-above the threshold value. Nevertheless, at least part of the plot can still be fitted with a linear dependence and the threshold can be extrapolated.

When using more radiation resistant material like Ce:YAG, the threshold energy can be easily crossed with mildly attenuated beam, as shown in Fig. 3(a). On the other hand, the information about the intensity distribution in the beam wings can be partially lost as the fluence in this region is not high enough to ablate the material even though the beam at full power is used. However, it was demonstrated before that the visibility of weak beam wings can be substantially increased in a suitable material with its post exposure development [33].

Results important for beam characterization were obtained also from fitting the merged data involving all the normalized f-scans, as shown in Fig. 7. Since the data from different f-scans follow the same trend and overlap with one another, this plot proves that the f-scan curve is independent from material properties. Moreover, all the extrapolated energy thresholds are very close to their real values. In addition, information from the high and low intensity part of the beam is shown on the same graph, since f-scans from different materials cover together a much wider range in damaged area, than each one of them individually. The effective beam area calculated from the plot in Fig. 7 was found to be 25.4 ± 3 μm^2, which is in very good agreement with all the previously reported values (see Table 1).

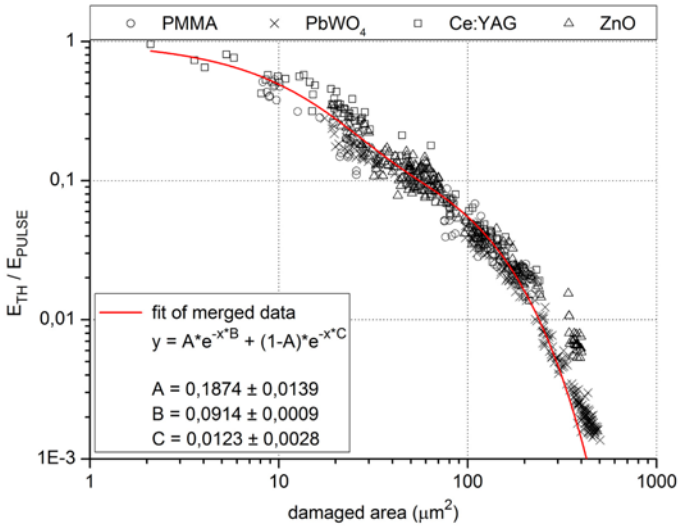

Fig. 7. Merged f-scans for all the irradiated materials and their fit.

4. Conclusions

The interaction of intense soft x-ray laser radiation with three inorganic scintillator materials (Ce:YAG, $PbWO_4$, and ZnO) was investigated. Threshold fluences required for irreversible surface change caused by a single ultra-short FEL pulse, were determined for three materials irradiated by focused beam of FLASH free-electron laser system tuned to the wavelength of 4.6 nm. The thresholds together with attenuation lengths indicate $PbWO_4$ as the material most sensitive to FEL soft x-rays among the three scintillation materials investigated. Comparison of normalized f-scans evaluated for all irradiated materials was performed. All values of

#224407 - $15.00 USD Received 9 Oct 2014; revised 15 Dec 2014; accepted 17 Dec 2014; published 7 Jan 2015

effective beam area derived from the f-scans are in very good agreement with the result obtained from the PMMA sample, which was used as a reference. Combining the f-scans obtained from different materials to improve accuracy and reliability of the effective beam area evaluation proved to be very effective. Hence, all three inorganic materials can be used for X-ray laser beam characterization based on ablative imprints. In addition, both remarkable etch rates and the clean character of ablation in various ionic crystals exposed to 4.6 nm laser radiation, strongly support the potential utilization of soft x-ray lasers for high aspect ratio micro(nano)processing and pulsed laser deposition of materials exhibiting a very weak linear absorption in the UV-Vis-NIR spectral regions.

Acknowledgments

This work was supported by the Czech Science Foundation under grant P108/11/1312. TB and MP appreciate funding provided by the Grant Agency of Charles University (project 1374213) and by the European Social Fund and the state budget of the Czech Republic (project CZ.1.07/2.3.00/30.0057) for their doctoral and postdoctoral fellowships, respectively. JCh thanks to the Academy of Sciences of the Czech Republic for a financial support of his postdoctoral position at the Institute of Physics. KS and PS are indebted to the Slovak Grant Agency for Science for financial support of VEGA Projects No. 2/0128/13 and No. 1/0148/12, respectively. Authors gratefully acknowledge the company Crytur (Turnov, Czech Republic) for the free supply of Ce:YAG crystals used in this experiment. SB would like to acknowledge funding provided by the Helmholtz Association through program-oriented funds.